Coloured TiO$_2$ based glazing obtained by spray pyrolysis for solar thermal applications

M. Dudita[a,*], L.M. Manceriu[b,1], M. Anastasescu[c], M. Nicolescu[c], M. Gartner[c], A. Duta[a,**]

[a]Transilvania University of Braşov, Renewable Energy Systems and Recycling Department, Eroilor 29, 500036 Braşov, Romania
[b]CNRS, Université de Bordeaux, ICMCB, 87 Avenue du Dr. Albert Schweitzer, F-33608 Pessac, France
[c]Institute of Physical Chemistry "Ilie Murgulescu", 202 Splaiul Independentei Street, 060021 Bucharest, Romania

Abstract

Titanium dioxide thin films with coloured reflections were deposited on glass substrate by robotic spray pyrolysis deposition using titanium (IV) isopropoxide as a precursor and air as a carrier gas. The films' optical properties were analyzed by UV–vis–NIR spectrometry using a 150 mm integrating sphere and spectroscopic ellipsometry (SE). The surface properties were evaluated by atomic force microscopy (roughness and morphology) and contact angle measurement (wettability). The colour variation of the films was determined in the CIE (Commission Internationale d'Eclairage) L*a*b* colour system by using the total reflectance spectra measured in the visible range.

Thin films with low roughness (< 4.5 nm), high transparency (> 70%) in the UV–vis–NIR region and hydrophilic properties were obtained. The optical properties, particularly transmittance are not influenced by humidity exposure. The colour of the films depends on the number of deposition sequences due to thickness and surface topology modification. By varying the deposition sequences brownish, purple, light-violet or purple–brown coloured reflections can be obtained. These coloured TiO$_2$ thin films will be used in solar collectors' glazing, supporting increased architectural acceptance.

© 2013 Elsevier Ltd and Techna Group S.r.l. All rights reserved.

Keywords: A. Films; C. Colour; D. TiO$_2$; Solar thermal collectors

1. Introduction

The future strategy towards 2020 outlines the need of thermal energy production on-site, based on renewables, and solar-thermal systems are among the most cited candidates. However, extended implementation of solar-thermal technologies in the built environment requires, besides high efficiency, increased architectural acceptance, particularly when targeting facades' integration. Different studies outlined the need for coloured collectors, more preferred than the usual black or dark blue ones, even if the conversion output was sometimes diminished [1]. Flat plate solar thermal collectors can be coloured by embedding a coloured absorber plate and/or by colouring/shading the glazing. While for the absorber plates plenty of coloured oxides can be recommended (CoO$_x$ [2,3] VO$_x$ [4], FeO$_x$ [5], etc.), only few economically viable solutions to increase the architectural attractiveness of solar collectors by using coloured glazing were found [6,7].

Recent studies have shown that thin films multilayers could be used to obtain coloured reflection due to interference [7]. The most important optimization criteria for the thin films used as collector glazing are the optical properties and stability in the working conditions, especially to condensed atmospheric vapours. The materials must have high transmittance in the incident (solar) radiation range and anti-reflexive properties. The main challenge is to control these parameters and to obtain reproducibility on large surfaces in cost-effective processes. The optical properties in the visible region can be tailored by controlling the film thickness, morphology or layer structure/composition as already shown by the recent studies on coatings based on titanium alloy nitride [8,9], zirconium oxynitride [10], NiO [11], mixed layers of SiO$_2$/TiO$_2$ [12] or polymers [13].

*Corresponding author. Tel.: +40 72 1781410.
**Corresponding author. Tel.: +40 72 3561089.
E-mail addresses: mihaela.dudita@unitbv.ro (M. Dudita),
a.duta@unitbv.ro (A. Duta).
[1]Present address.

The use of pristine TiO_2 represents another option, due to the versatility of this material, with very good optical properties and stability [14]. The need of solar-thermal collectors integrated in facades is of recent date, therefore coloured glazing, based on efficient and low cost solutions (as single TiO_2 is) are scarce, and there are even less reports on the evaluation of the chromaticity parameters [15].

Various techniques are used to obtain thin films including physical and chemical techniques [16–19]. Among these, spray pyrolysis deposition (SPD) is commonly used for the development of commercial window glasses. The SPD technique is a low cost method, easy up-scalable. It can be applied on surfaces with various geometries while preserving good control over the properties.

The paper presents novel results on coloured glazing based on TiO_2 thin films outlining that the apparent colour of the films can be easily modified by varying the thickness and morphology in a multi-layered structure. The aim is to investigate the influence of the deposition parameters on the surface properties of the coloured thin films obtained using SPD. To the best of our knowledge, it is the first time that coloured TiO_2 thin films are reported to be obtained by robotic spray pyrolysis with application in solar collectors' glazing.

2. Experimental

For the deposition of the coloured TiO_2 films, ethanolic (EtOH) solutions of titanium (IV) isopropoxide (TTIP) and 2,4-pentanedione (AcAc) were used.

Microscopic glass was chosen as substrate for the deposition of the coloured thin films. In solar thermal flat plate collectors, the standard glazing consist of highly textured solar glass; thus, the microscopic glass can be used as reference (worst case scenario), and further up-scaling using solar glass can only intensify the colour/shading effect due to interference fringes. Additionally, the high roughness of the solar glass may raise certain experimental issues in some characterization processes like ellipsometry. Therefore, microscopic glass was preferred in the optimization process.

The TiO_2 thin films were deposited by robotic spray pyrolysis deposition. The deposition parameters were optimized to obtain thin, uniform films as follows: spraying solution composition TTIP:AcAc:EtOH=1:1.5:22.5, deposition temperature (T)= 450 °C, airflow pressure (p)=1.4 bar, break between two consecutive spraying sequences: 70 s. Different film thicknesses and thus different coloured reflections were obtained by varying the number of spraying sequences. The samples were labelled with T_x, were x is the number of consecutive spraying sequences.

Flat plate collectors are not completely tide, and water vapours can diffuse inside during the hot days when the sealing is more permeable, while during nights, the vapours condense on the glazing. Therefore, the stability in wet environments of the glazing coating (TiO_2 thin films) should be assessed. To accelerate the possible destructive process, the TiO_2 samples were immersed in purified water for 2 h at 40 °C, and the optical properties were evaluated before and after the test.

The crystalline composition in the films was assessed by X-ray diffraction (XRD, Bruker D8 Discover). However, all the films are amorphous, and no anatase (or other polymorph) was detected. The films morphologies were studied using Atomic Force Microscopy (AFM, XE-100 model from Park Systems). The images were taken in non-contact mode with Si-tips (PPP-NCLR type from Nanosensors™ < 8 nm tip radius) of app. 225 μm length, 38 μm width and 48 N/m spring constant/∼190 kHz resonance frequency. The topographical 2D AFM images were taken over the area of 1×1 μm^2, and tilt correction was performed before statistical data analysis, including the calculation of the root mean square (RMS) roughness and skewness (S_{sk}) of the measured region. Spectroscopic ellipsometry (SE) measurements were performed by a VASE-Woollam equipment. Ellipsometric parameters ψ (the rotation angle of the polarizer) and Δ (the rotation angle of the analyzer) were registered in the 250–1700 nm range, at 70° angle of incidence, 10 nm step, 50 revolutions/step. The Cauchy model was used to fit the experimental data [20]. From the best fit, the thickness and the optical constants (n, k) of the films were calculated.

The optical properties of the films (transmittance, reflectance) were evaluated using UV–vis–NIR spectrometry (spectrometer Lamda 950 Perkin-Elmer, equipped with a 150 mm integrating sphere).

The colour variation of the films was evaluated in the CIE (Commission Internationale d'Eclairage) L*a*b* colour system by using the total reflectance spectra in the visible range (400–700 nm). The colour of a surface was computed for a 10° observer (CIE 1964) and D-65 illuminant. In particular, L* represents the lightness of the sample, a* and b* are the chromatic coordinates, respectively varying between green (−a*) and red (+a*) and between blue (−b*) and yellow (+b*) [21]. According to the CIE method the tristimulus values for a 10° observer (CIE 1964) and D-65 illuminant are derived from the colour reflectance spectra [21,22].

3. Results and discussions

3.1. Optical properties – UV–vis–NIR

Samples with different TiO_2 film thicknesses were deposited using the optimized SPD deposition parameters. The TiO_2 thin films will be used as coloured glazing; thus the optical properties of the films were primarily evaluated. The total transmittance was determined in the range 250–2500 nm, using a 150 mm integrating sphere, at normal incidence and at 15° (Fig. 1).

Considering that the solar thermal conversion consists of two mechanisms, i.e. conversion of the incident UV–vis radiation into heat and NIR radiation transmission (convection), the optimized materials for the solar glazing should have high transmittance over the entire UV–vis–NIR range. Coloured films have a slightly decreased visible transmittance compared to the glass substrate; but it still good, above 80% (Fig. 1). Additionally, 40% of incident radiation is in the NIR spectral range. Therefore, it is still possible to have an adequate amount of radiation reaching
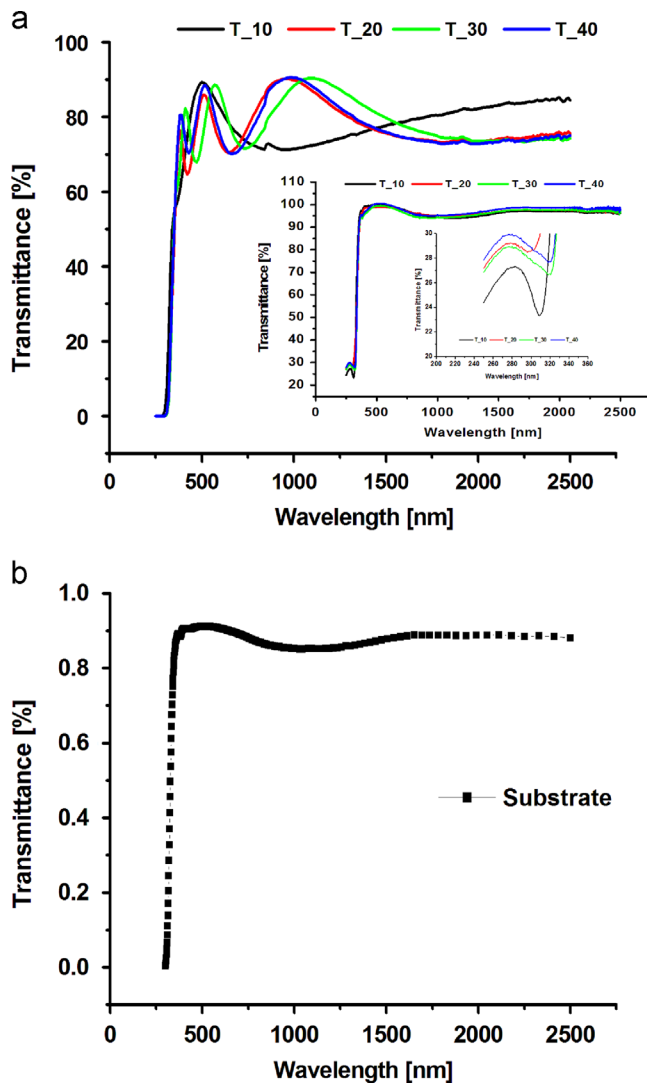
Fig. 1. Normal incidence and 15° transmittance spectra (in the inset) of the TiO$_2$ films obtained by varying the number of deposition sequences (a) and for the substrate (b).

The diffuse reflectance was measured by using a light trap at the specular reflectance angle. All the samples present very low diffuse reflectance (< 2%), matching the requirements for quality glazing. The surface roughness is also expected to be reduced. The samples are characterized by low total reflectance values, a compulsory condition for materials used as transparent glazing in solar collectors (Fig. 2). The number of the interference fringes is increasing with the number of deposition sequences, influencing the films' colour. This confirms the layer-by-layer (Frank-van der Merwe) growth mechanism involved in the formation of the TiO$_2$ layers deposited with 20 and 30 spraying sequences.

Titanium oxide colours are indeed due to interference phenomena at the air/metal oxide/substrate interfaces, as confirmed by the interference fringes composing the transmission and reflectance spectra (Figs. 1 and 2, respectively). The brightness of the layers slightly increases with the film thickness as the layer homogeneity is improved and consequently
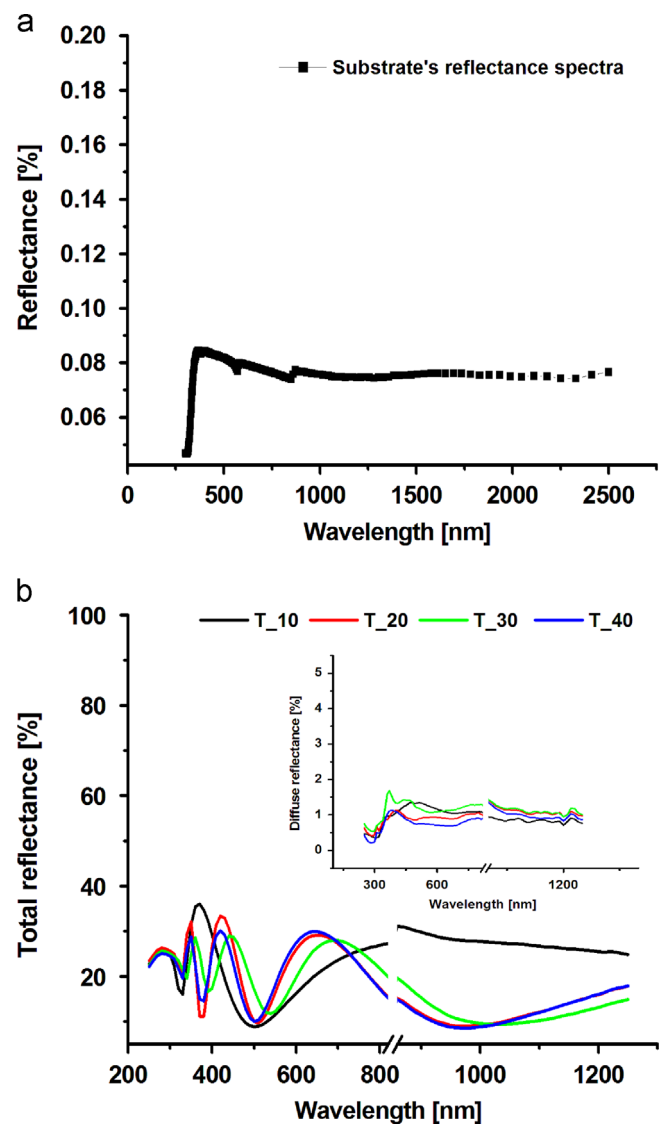
the absorber when using coloured glazing, as the NIR transmittance is well supported. Following the different characteristics of the transmission spectra for the normal and 15° incidence angle, the TiO$_2$ films will have different colours depending on the thickness and the incidence angle. This may be explained by the waviness of surface that induces differences in the interaction of radiation with the film surface. It is also notable that, as result of the deposition conditions with quite significant breaks between the spraying sequences, the film is actually a multi-layered structure, additionally promoting multiple reflections and interference. The oscillations recorded in the visible range (Fig. 1) are the result of the optical interference caused by the differences in the refraction indexes (n) of the substrate and of the film. These oscillations also confirm the possible slight variations in the interlayers (with different local densities) of n, and the multiple reflections occurring on and in the upper layers of the film. The sharp slope corresponds to the fundamental absorption edge of TiO$_2$ which is red shifted (due to scattering) when increasing the number of the spraying sequences and the film thickness.

Fig. 2. The substrate's total reflectance (a) and the total and diffuse reflectance (in the inset) of the TiO$_2$ films obtained by varying the number of deposition sequences (b).

radiation loss through diffusion is diminished (inset of Fig. 2). The red contribution (a*) is rather constant, whereas the blue component (b*) variation mainly determines the perceived layer colour. The theoretical colours of the samples were computed with the EasyRGB online software application [23], using the calculated L*, a* and b* parameters and also shown in Fig. 3. As the number of spraying sequences increases b* acquires a more negative value, giving sample T_30 a more bluish appearance. It was reported that colour change can be related also to the surface stoichiometry modification [24]. The deposition conditions of the thin films involve rather high temperature and air flow pressure leading to a lower amount of oxygen vacancies (due to passivation). Additionally, the stoichiometry was controlled by varying and optimizing the break duration between the spraying sequences, which allows by-products elimination and oxygen migration in and out of the film until an equilibrium, stabile composition is reached, as already Ayouchi et al. [25] showed for ZnO thin films with increased stoichiometry, obtained via SPD at higher deposition temperatures. No annealing treatment was applied to the as deposited films as the aim is to develop a low energy consuming technology.

3.2. Film thickness measurement – spectroscopic ellipsometry analysis results

The film's thickness was evaluated using spectroscopic ellipsometry (SE) analysis. The SE method is an optical, non-destructive and contactless technique for the investigation of the dielectric properties (complex refractive index) of thin films.

The film's thickness and surface roughness can be evaluated based on different optical models [26,27], and considering the results, a two layer model was used to fit the ellipsometric data. For the TiO$_2$ film and for the roughness layer simulation, the Cauchy model [28] and, respectively, the Bruggeman Effective Medium Approximation [29] with 50% TiO$_2$ and 50% air were applied. The ellipsometric measurements together with the best fit are presented in Fig. 4 for the sample T_20. Fitting errors ranged from 5.97% for the T_10 sample, up to 12.00% for sample T_40, confirming the stacked layers structure of the films.

The layer thicknesses and refractive index were obtained from the best fit at the 550 nm wavelength, and their variation with the number of deposition sequences is presented in Fig. 5a.
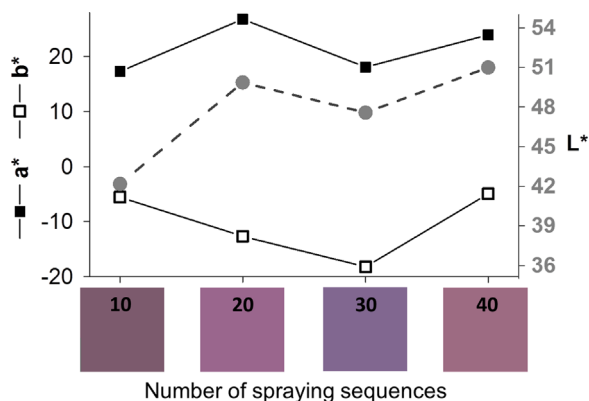

Fig. 3. CIEL*a*b* colour coordinates versus the number of deposition sequences.
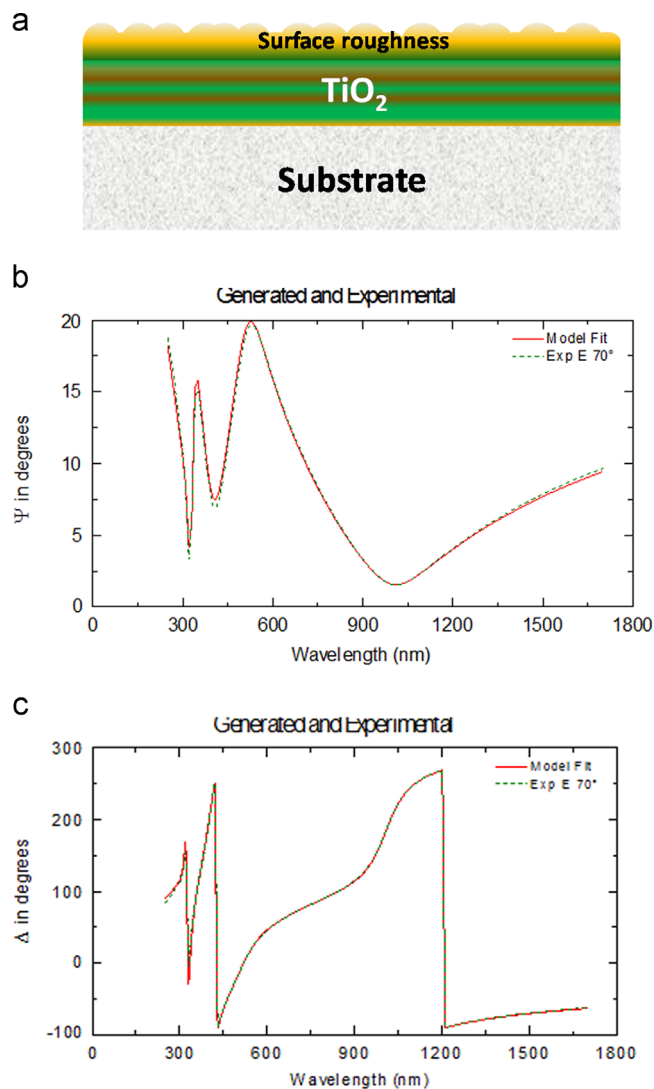

Fig. 4. The experimental data, the model (a) used and the fitted spectra of the ellipsometric parameters Ψ (b) and Δ (c) corresponding to sample T_20.

The TiO$_2$ film thickness increases with the deposition sequences, but not linearly, because after the first deposition, the film is not fully stabilized. After the second and following depositions, the film resident on the heater can be subject to in situ annealing followed by densification as result of aggregates re-organization. Thus the film thickness slowly decreases (Fig. 5a). A positive result is that all these films are not absorbing in the 400–1700 nm range (k=0, Fig. 5b), and the films get improved optical stability after 30 deposition sequences, confirmed by the rather constant overall n values.

The packing density was calculated using the Lorentz-Lorenz formula (Eq. 1, [30]), where s and n is the refractive index of the substrate and of the film, determined from the SE analysis.

$$p = \frac{(s^2+1)(n^2-1)}{(s^2-1)(n^2+1)} \tag{1}$$

The packing density is slightly lower for the sample T_10 (1.7169), but after 20 spraying sequences the film density
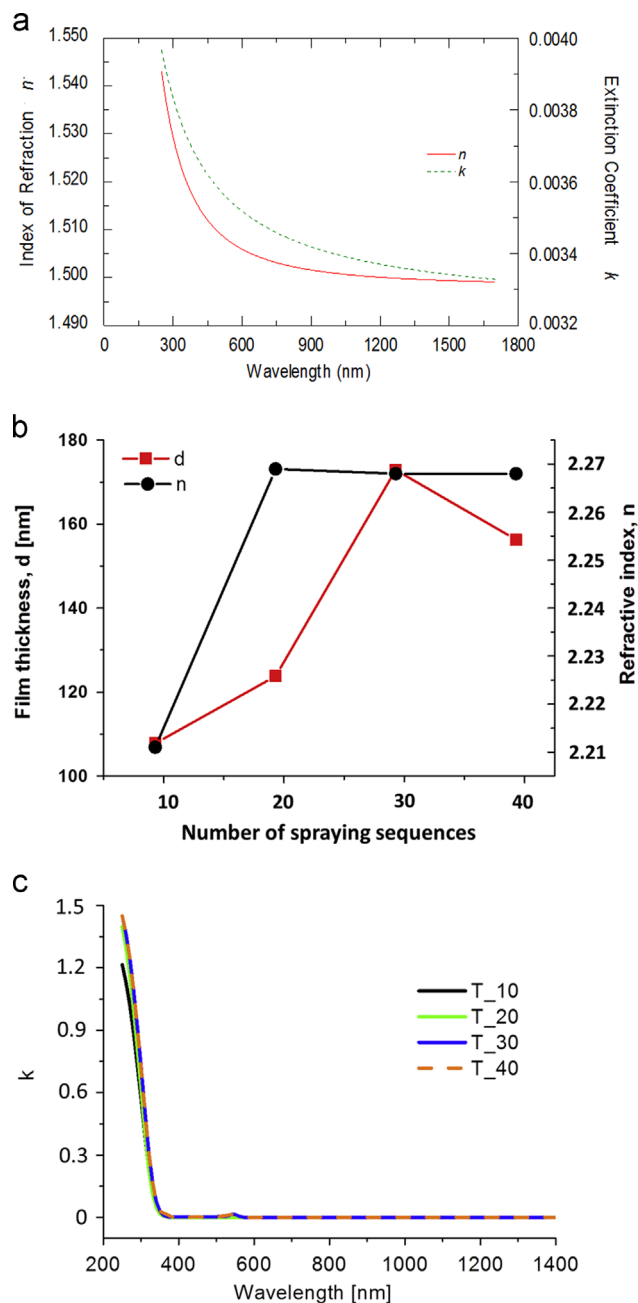
Fig. 5. Substrate's optical properties determined by spectroscopic ellipsometry (a); thickness and refractive index variation with the number of deposition sequences (b) and extinction coefficient dispersion with wavelength (c) for the TiO$_2$ samples.

reaches a constant value (1.7536–1.7536) proving that the film structure is stabilized. The surface roughness values evaluated using spectroscopic ellipsometry support this affirmation, decreasing from 3.6–3.9 nm for samples T_10, T_20, and T_30 down to 2.1 nm for sample T_40.

3.3. Morphology and contact angle measurements

Following the aggregates reorganization, varying the number of deposition sequences modifies not only the film thickness but also the surface profile (Fig. 6). Root mean roughness (RMS) and surface skewness (S_{sk}) were evaluated using the AFM software for a 1 μm × 1 μm surface and plotted versus the deposition sequences (Fig. 6d). The films are very smooth with roughness values in the range of 0.5–1.6 nm (Fig. 7d), slightly lower than the values obtained from the SE analysis. Roughness values from SE could be compared [31] with the AFM ones using the correlation roughness $_{AFM} = 1/2$roughness$_{SE}$. The negative skewness values (Fig. 6d) confirm that films are reached in pores [32], and the most negative value corresponds to sample T_40 which has the highest pores density. After 10 deposition sequences, the morphology of the films (Fig. 6a) was rather textured, characterized by large open pores and a random aggregates distribution.

The film growth rate was plotted versus the number of deposited sequences (Fig. 7) and used to explain the topology and thickness changes which were consequences of the processes involved in film formation.

A mechanism of film growth depending on the number of deposited sequences is proposed and schematically described in Fig. 7. The following steps described the various growth stages depending on structural conditions and temperature, and only the ones likely to prevail are further discussed, correlated with the number of spraying sequences.

Initially, the precursor species adsorb on the substrate (I) where decomposition/reaction takes place. At the beginning, isolated tri-dimensional nuclei are formed which increase in size and number (Volmer–Weber growth mechanism). Their distribution on the substrate is not only influenced by the properties of the Taylor spraying cone (number and size of the aerosol and its speed), but is also diffusion controlled (II). As the substrate is highly smooth, diffusion/wetting is less supported. Diffusion in the 2D (x, y) direction can be increased by spraying at a lower incidence angle (optimized at 45°). Grain growth (III) occurs by particle coalescence as the interatomic interactions between the precursor particles overcome those between precursor and substrate. Incomplete particle coalescence and grain boundary migration lead to the formation of a continuous film. Crystal growth (IV) follows with the new species bonding to the existing nuclei in random directions thus explaining the textured morphology of sample T_10 (Fig. 6a). This morphology scatters the incident light explaining why sample T_10 has the highest diffuse reflectance (Fig. 2). This is also in agreement with the chromaticity analysis which shows that sample T_10 has the lowest L* value. For the first deposition sequences, the nucleation and growth are the predominant process.

During the break between the spraying sequences, volatile by-products are removed (V); if the break between spraying is too low, the by-products can be partially trapped in the film leading to uncontrolled results, [33,34]. The break between sequences must be optimized and take into consideration the time needed for re-heating the substrate, locally cooled by the aerosol droplets. Increased break (and SPD) duration supports the structure densification (Fig. 6b, c) and uniform surface energy distribution. At this point, a layer-by-layer (Frank and Vander Merwe) growth mechanism is favoured
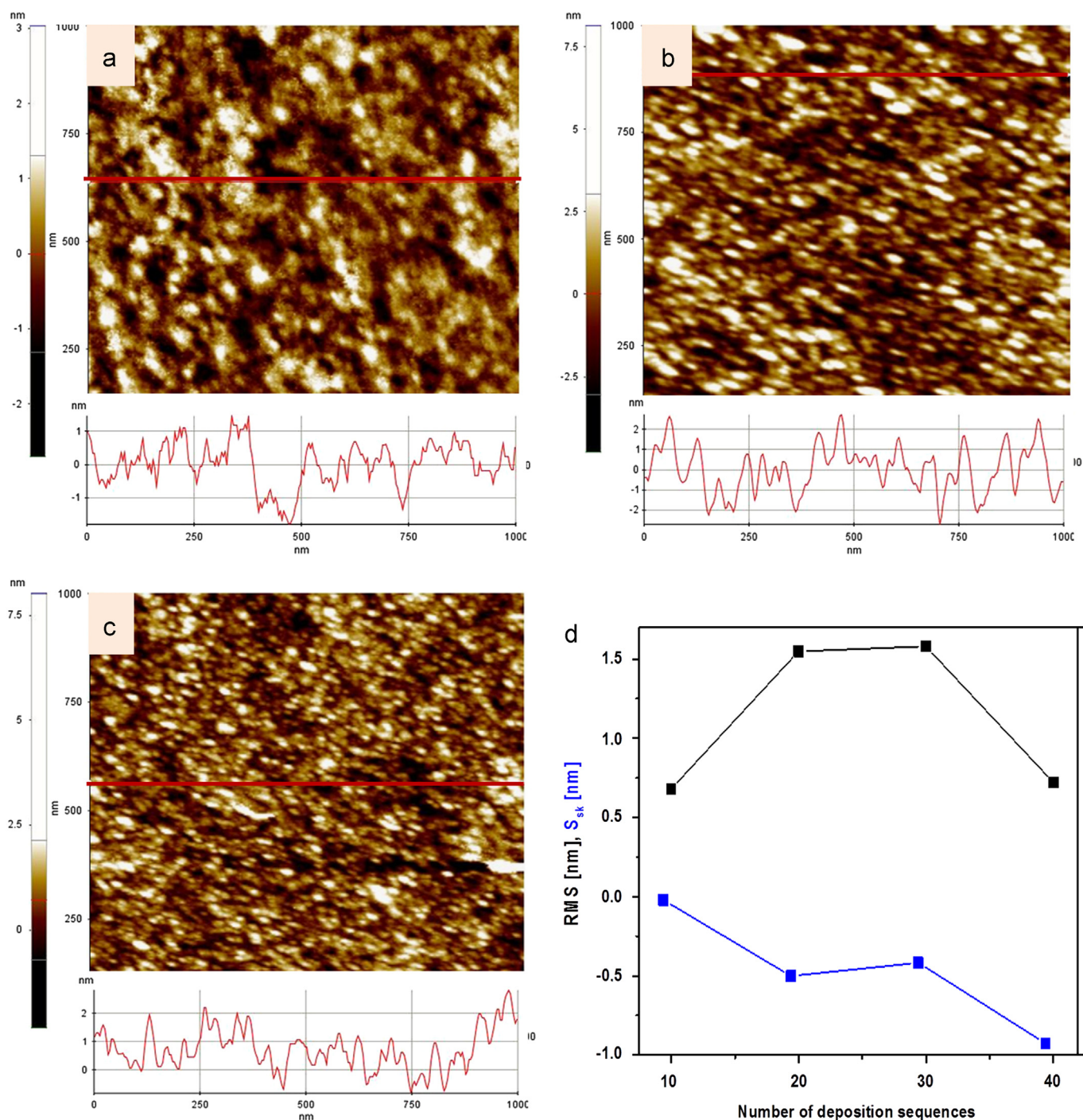
Fig. 6. AFM image of the samples T_10 (a), T_20 (b) and T_40 (c) and variation of root mean square roughness (RMS) and skewness (S_{sk}) with number of deposited sequences (d).

with new ad-atoms bonding preferential to the top of already formed crystals (IV) forming monoatomic layers and encouraging the growth in the z-direction but with a lower rate (Fig. 7). This is confirmed by the increase in the layer thickness and number of interference fringes for samples T_20 and T_30. Although still present, surface diffusion (II) and particle reorganization (III) have a minor contribution in this stage as surface mobility is decreased. Sample T_30 presents a similar morphology with sample T_20 as

confirmed also by the roughness and skewness values; therefore, it was not presented. However, with increasing the number of deposited layers, the surface concentration of the species has lower variations, the surface energy decreases, and the growth rate reaches a minimum after 40 spraying sequences (Fig. 7). Concluding, the complete particle coalescence with grain boundary diffusion (III) and by-products desorption (V) are the main processes influencing the film structure, supported by the prolonged deposition
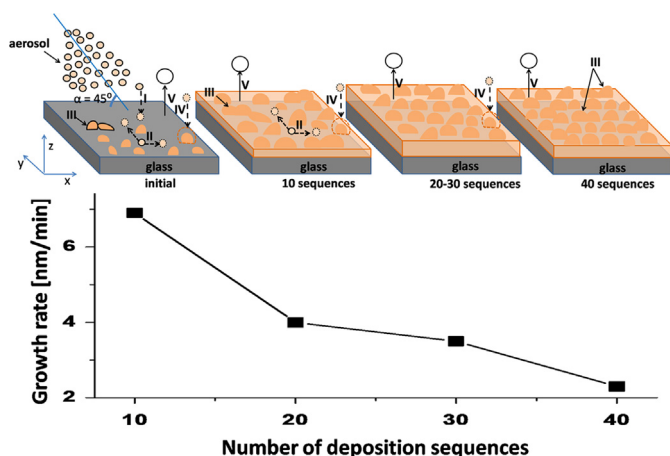
Fig. 7. TiO$_2$ film growth rate as function of number of deposition sequences and processes involved in film formation.

Table 1
Contact angle measurement results.

Sample	Water contact angle [degree] and droplet profile on the surface	
T_10	25.7	
T_20	33.05	
T_30	34.4	
T_40	35.5	

time. This is confirmed by film thickness which shows no important modification after 30 sequences (Fig. 6a).

The AFM images confirm that film uniformity is improved with increasing the number of deposition sequences; sample T_40 is characterized by a homogenous distribution of particles and pores over the surface (Fig. 6c). We can conclude that surface morphology mainly influences the L* parameter. Still, there is a limit in the number of spraying sequences above which the layer thickness significantly influences the heat transferred to the incoming ad-atoms and the diffusion properties in the film and thus the growth mechanism of the thin layers.

As the TiO$_2$ thin films will be used for solar collector glazing where condensation frequently occurs, the amount of the reflected radiation when water condenses on the film should be minimal. When water lays on the surface wetting behaviour is preferred, with a continuous layer as compared to multiple drops to avoid light scattering on the droplets and thus to obtain low radiation losses. Therefore, initial contact angle values were measured for water, and the values are given in Table 1. The values range from 25.7 to 35.5°, proving the hydrophilic character and the increased wettability of the films; the values for the initial water contact angle are slowly increasing with the number of spraying sequences most probably because of film superficial densification. The lowest water contact angle (25.7°) is observed for the sample obtained by 10 deposition sequences characterized by non-homogeneous surface with large open pores on the surface (Fig. 6a). Sample T_40 has the highest water contact angle value (35.5°) in agreement with the AFM data (Fig. 6c). In this case, the morphology seems more closely packed and the samples have the lowest roughness [35].

3.4. Stability in wet conditions

The TiO$_2$ thin films should be stable in the outdoor environment and should withstand prolonged exposure to humidity, meaning that the layer composition and surface must not change. Considering the working environment of the

solar collectors, especially the thin condensed vapours' layers on the glazing, the stability of the TiO$_2$ thin films was further assessed in direct contact with water. The samples were immersed in purified water and the transmission spectra at 15° incidence angle were registered before and after the tests. The spectra are shown in Fig. 8. All the samples have high transmittance values in the near infrared region, similar with the initial values (T_10, T_30) or slightly higher (T_20, T_40), proving a conditioning effect.

In the UV–vis domain the absorption maxima change and the interference fringes number is diminished suggesting that a change might have occurred in the morphology of the super-ficial layer. This means that the thin layers predominantly reflect a single colour at normal incidence angle. From the transmission spectra, it can be seen that the TiO$_2$ characteristic absorbing edge is not shifted. It can be concluded that the obtained TiO$_2$ glazing fits well with the targeted application as it allows the solar radiation (including heat) to pass through the glass cover thus contributing to the "greenhouse effect" inside and does not significantly modify the optical properties when exposed to humidity, allowing the optimum solar-thermal conversion efficiency to be achieved.

4. Conclusions

TiO$_2$ thin films with good optical properties (high transparency in the 350–2500 nm range) and low roughness (< 4.5 nm) were obtained by spray pyrolysis deposition. The extinction coefficient shows only slight variation with the number of spraying sequences. The colour coordinates of the TiO$_2$ thin films obtained by SPD were for the first time studied in the CIEL*a*b* system. The films colour varies with the number of deposition sequences due to thickness and surface topology modification. As optimized, the break between the spraying sequences allows a multi-layered structure, with gradient density that additionally supports the multiple reflections inside the thin films. The results are small variations in the refractive index, leading to an instrument in tailoring the coloured reflection of the films. Thus, varying the deposition sequences, brownish, purple, light-violet, or purple–brown coloured reflections were obtained. The TiO$_2$ coatings
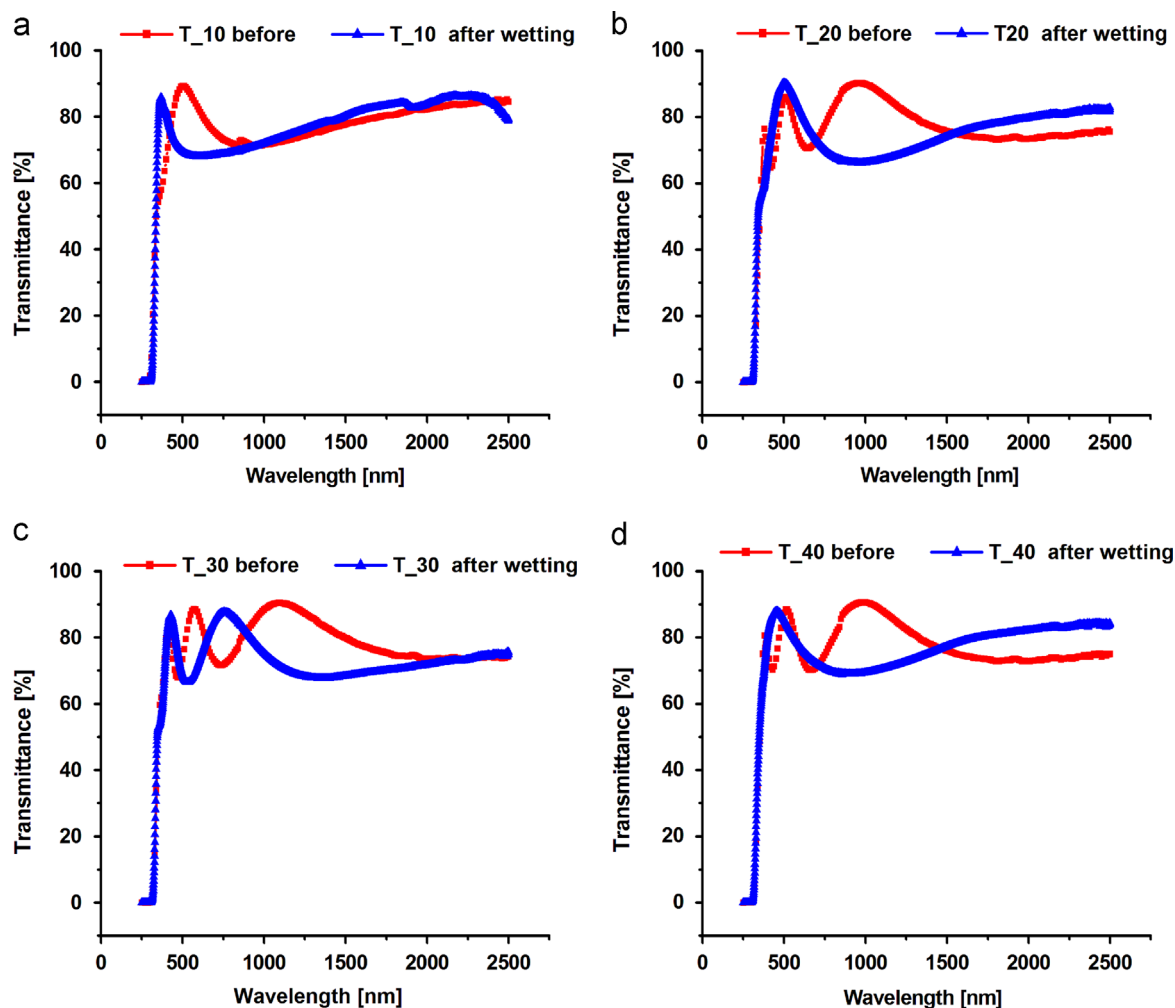
Fig. 8. Transmission spectra of the samples T_10 (a), T_20 (b), T_30 (c) and T_40 (d) before (red line) and after wetting (blue line) registered at 15° incidence angle. (For interpretation of the references to colour in this figure legend, the reader is referred to the web version of this article.)

show a hydrophilic character, slowly decreasing with the number of deposited sequences, but the optical properties are not influenced by humidity exposure.

Acknowledgment

References

[1] M.C. Munari Probst, C. Roecker, Architectural Integration and Design of Solar Thermal Systems, EPFL Press, Lausanne, 2011.

[2] A. Amri, X. Duan, C.-Y. Yin, Z.-T. Jiang, M.M. Rahman, T. Pryor, Solar absorptance of copper–cobalt oxide thin film coatings with nano-size, grain-like morphology: optimization and synchrotron radiation XPS studies, Applied Surface Science 275 (2013) 127–135.

[3] S. Meseguer, M.A. Tena, C. Gargori, R. Galindo, J.A. Badenes, M. Llusar, G. Monrós, Development of blue ceramic dyes from cobalt phosphates, Ceramics International 34 (2008) 1431–1438.

[4] P. Liu, S-H. Lee, C.E. Tracy, J.A. Turner, J.R. Pitts, S.K. Deb, Electrochromic and chemochromic performance of mesoporous thin-film vanadium oxide, Solid State Ionics 165 (2003) 223–228.

[5] S. Park, Preparation of iron oxides using ammonium iron citrate precursor: thin films and nanoparticles, Journal of Solid State Chemistry 182 (2009) 2456–2460.

[6] A. Schüler, C. Roecker, J.-L. Scartezzini, J. Boudaden, I.R. Videnovic, R.S.-C. Ho, P. Oelhafen, On the feasibility of colored glazed thermal solar collectors based on thin film interference filters, Solar Energy Materials and Solar Cells 84 (2004) 241–254.

[7] S. Mertin, V. Hody-Le Caër, M. Joly, I. Mack, P. Oelhafen, J.-L. Scartezzini, A. Schüler, Reactively sputtered coatings on architectural glazing for coloured active solar thermal façades, Energy and Buildings, http://dx.doi.org/10.1016/j.enbuild.2012.12.030, in press.

[8] J.-M. Chappé, N. Martin, J. Lintymer, F. Sthal, G. Terwagne, J. Takadoum, Titanium oxynitride thin films sputter deposited by the reactive gas pulsing process, Applied Surface Science 253 (2007) 5312–5316.

[9] J.H. Lee, G.E. Jang, Y.H. Jun, Investigation and evaluation of structural color of TiO_2 coating on stainless steel, Ceramics International 38S (2012) S661–S664.

[10] F. Vaz, P. Carvalho, L. Cunha, L. Rebouta, C. Moura, E. Alves, A. R. Ramos, A. Cavaleiro, P.H. Goudeau, J.P. Rivière, Property change in ZrN_xO_y thin films: effect of the oxygen fraction and bias voltage, Thin Solid Films 469–470 (2004) 11–17.

[11] D.S. Dalavi, M.J. Suryavanshi, S.S. Mali, D.S. Patil, P.S. Patil, Efficient maximization of coloration by modification in morphology of

electrodeposited NiO thin films prepared with different surfactants, Journal of Solid State Electrochemistry 16 (2012) 253–263.

[12] A. Schüler, C. Roecker, J. Boudaden, P. Oelhafen, J.-L. Scartezzini, Potential of quarterwave interference stacks for colored thermal solar collectors, Solar Energy 79 (2005) 122–130.

[13] R.J. Mortimer, K.R. Graham, C.R.G. Grenier, J.R. Reynolds, Influence of the film thickness and morphology on the colorimetric properties of spray-coated 16 electrochromic disubstituted 3,4-propylenedioxythiophene polymers, ACS Applied Materials and Interfaces 1 (2009) 2269–2276.

[14] J. Boudaden, P. Oelhafen, A. Schüler, C. Roecker, J.-L. Scartezzini, Multilayered Al_2O_3/SiO_2 and TiO_2/SiO_2 coatings for glazed colored solar thermal collectors, Solar Energy Materials and Solar Cells 89 (2005) 209–218.

[15] M.V. Diamanti, B. Del Curto, M. Pedeferri, Interference colors of thin oxide layers on titanium, Color Research and Application 33 (2008) 221–228.

[16] C.J. Tavares, S.M. Marques, L. Rebouta, S. Lanceros-Méndez, V. Sencadas, C.M. Costa, E. Alves, A.J. Fernandes, PVD-grown photocatalytic TiO_2 thin films on PVDF substrates for sensors and actuators applications, Thin Solid Films 517 (2008) 1161–1166.

[17] P. Piszczek, Ż. Muchewicz, A. Radtke, M. Gryglas, H. Dahm, H. Różycki, CVD of TiO_2 and TiO_2/Ag antimicrobial layers: deposition from the hexanuclear μ-oxo Ti(IV) complex as a precursor, and the characterization, Surface and Coatings Technology 222 (2013) 38–43.

[18] W. Du, Y. Ye, H. Li, F. Zhao, L. Ji, W. Quan, J. Chen, H. Zhou, Low temperature preparation of transparent, antireflective TiO_2 films deposited at different O_2/Ar ratios by microwave electron cyclotron resonance magnetron sputtering, Vacuum 86 (2012) 1387–1392.

[19] J. Krýsa, P. Novotná, Š. Kment, A. Mills, Effect of glass substrate and deposition technique on the properties of sol gel TiO_2 thin films, Journal of Photochemistry and Photobiology A 222 (2011) 81–86.

[20] H.G. Tompkins, WVASE32 Software Training Manual, J.A. Woollam Co., Inc., 2006.

[21] J. Schanda, Colorimetry. Understanding the CIE System, John Wiley & Sons, Hoboken, 2007.

[22] A.R. Zarubica, M.N. Miljcović, M.M. Purenović, V.B. Tomić, Color parameters, whiteness indices and physical features making paints for horizontal signalization, Facta Universitatis Series: Physics Chemistry and Technology 3 (2005) 205–2016.

[23] ⟨www.easyrgb.com⟩.

[24] K. Narasimha Rao, Influence of deposition parameters on optical properties of TiO_2 films, Optical Engineering 41 (2002) 2357–2364.

[25] R. Ayouchi, F. Martinb, D. Leinena, J.R. Ramos-Barrado, Growth of pure ZnO thin films prepared by chemical spray pyrolysis on silicon, Journal of Crystal Growth 247 (2003) 497–504.

[26] Hiroyuki Fujiwara, Spectroscopic Ellipsometry: Principles and Applications, Willey, 2007.

[27] M. Gartner, A. Szekeres, P. Osiceanu, M. Anastasescu, M. Stoica, A. Marin, E. Vlaikova, E. Halova, Infrared ellipsometry as an investigation tool of thin layers grown into plasma immersion N^+ implanted silicon, Applied Surface Science 258 (2012) 7195–7201.

[28] H.G. Tompkins, E.A. Irene, Handbook of Ellipsometry, William Andrews Publications, Norwich, NY, 2005.

[29] D.A.G. Bruggeman, Berechnung verschiedener physikalischer Konstanten von heterogenen Substanzen, Annals of Physics 24 (1935) 636–679.

[30] S.D. Ventura, E.G. Birgin, J.M. Martínez, I. Chambouleyron, Optimization techniques for the estimation of the thickness and the optical parameters of thin films using reflectance data, Journal of Applied Physics 97 (2005) 043512.

[31] D.E. Aspnes, J.B. Theeten, F. Hottier, Physical Review B20 (1979) 3292.

[32] A. Mendez-Vilas, J.M. Bruque, M.L. Gonzalez-Martin, Sensitivity of surface roughness parameters to changes in the density of scanning points in multi-scale AFM studies. Application to a biomaterial surface, Ultramicroscopy 107 (2007) 617–625.

[33] C. Norton, Ceramic Materials. Science and Engineering, Springer, New York, 2007.

[34] M. Dudita, L. Isac, A. Duta, Influence of solvents on properties of solar selective coatings obtained by spray pyrolysis, Bulletin of Material Science 35 (2012) 997–1002.

[35] A.W. Neumann, R.J. Good, Surface and Colloid Science, vol. II, Plenum Press, New York, 1979.